ADVANCED MATERIALS INTERFACES
Open Access
www.advmatinterfaces.de

Omniphobic Photoresist-Assisted Patterning of Porous Polymethacrylate Films

*Dmitrii D. Kartsev, Ilia M. Lukianov, Eduard G. Sharapenkov, Artur Yu. Prilepskii, and Pavel A. Levkin**

Patterning of various surface properties, including roughness, wettability, adhesiveness, and mechanical properties, can markedly enhance the functionality of test systems. Thus, porous polymethacrylates prepared by polymerization-induced phase separation (PIPS) represent a promising class of functional materials for the construction of miniaturized test systems. Different porosity, surface chemistry, and wettability are achieved in porous polymethacrylates with different precursor compositions. Nevertheless, only wettability microstructuring has been highlighted for these materials thus far. Here, the study presents a novel method for the direct and selective deposition of porous polymethacrylate films with different surface chemistry and porosity. The selective adhesion of omniphobic–omniphilic wettability patterns is used to facilitate the polymer pattern formation. The feasibility of patterning with different monomers and porogenic solvents is demonstrated. The topological study confirms the selective application of polymer structures with different thickness and roughness. The wettability characterization of the omniphobic material shows no significant changes caused by the operations performed. Thus, a new pattern with a greater difference in the wettability of the areas is produced in the process. Discontinuous dewetting of different liquids is performed. The use of poly(2-hydroxyethyl methacrylate-co-ethylene dimethacrylate) (HEMA-EDMA) modified patterns for precise living cell patterning is also demonstrated.

1. Introduction

Microstructuring surface properties have effectively miniaturized test systems. For example, patterning of cell adhesive properties can be used to control cell apoptosis.[1] Wettability microstructuring is crucial for producing liquid droplet microarrays (DMA), which have proven effective for miniaturizing various chemical and biological experiments.[2,3] Patterning of various surface properties, including roughness, wettability, adhesiveness, and mechanical properties, can significantly enhance the functionality of test systems. Surface roughness correlates with cell and bacterial adhesion, necessitating specific substrate roughness for various experiments.[4] Specific surface roughness can inhibit the differentiation of pluripotent embryonic stem cells.[5] Defined roughness and wettability contrasts have been achieved using porous polymethacrylates produced by polymerization-induced phase separation (PIPS).[6,7] However, previous works focused on chemical patterns to control different properties, as patterning roughness was not feasible. Creating micropatterns of surfaces with different roughness is challenging but essential due to their diverse biological properties, local increase in specific surface area, and influence on wettability.

PIPS-derived porous polymethacrylates exhibit a wide range of applications due to the diversity of their porosity, surface chemistry, and wettability, which are influenced by the composition of the polymer precursors.[6] While wettability microstructuring has been reported for this class of materials,[7,8] roughness patterning has not yet been highlighted. The reason is that PIPS technique requires an oxygen-free environment. Therefore, when producing

D. D. Kartsev, I. M. Lukianov, E. G. Sharapenkov, A. Y. Prilepskii
International Institute "Solution Chemistry of Advanced Materials and Technologies" (SCAMT)
ITMO University
9 Lomonosova St., St. Petersburg 191002, Russia

The ORCID identification number(s) for the author(s) of this article can be found under https://doi.org/10.1002/admi.202400569

DOI: 10.1002/admi.202400569

P. A. Levkin
Institute of Biological and Chemical Systems – Functional Molecular Systems (IBCS-FMS)
Karlsruhe Institute of Technology (KIT)
Hermann-von-Helmholtz-Platz 1, 76344 Eggenstein-Leopoldshafen, Germany
E-mail: levkin@kit.edu

P. A. Levkin
Institute of Organic Chemistry (IOC)
Karlsruhe Institute of Technology (KIT)
Kaiserstraße 12, 76131 Karlsruhe, Germany

polymethacrylate structures, it is necessary to use molds that protect the precursor solution from exposure to atmospheric oxygen. Obtaining wettability patterns is possible in this case with surface chemical modification of the porous framework using photografting[7,9] and other methods.[10] It is worth noting that this approach is suitable for wettability patterning or for immobilization of different functional groups, but it is not useful for local control of roughness and porosity. Yet, there has been no method for direct application of porous polymethacrylates as a pattern. Herein we introduce a new method for the direct and selective deposition of porous polymethacrylate films. Our approach is based on the use of omniphobic–omniphilic wettability patterns to facilitate selective adhesion of porous polymethacrylate films. The proposed method reveals the whole potential of porous polymethacrylates and enables patterning of wettability, roughness, and surface chemistry.

Recently, we have shown the advantageous properties of the omniphobic photoresist based on polydimethylsiloxane-modified octaglycidyl polyhedral oligomeric silsesquioxane (GPOSS-PDMS) for wettability pattern formation.[11] Omniphobic surfaces are repellent to both water and low surface tension liquids, exhibiting low contact angle hysteresis and low sliding angles for water and liquids with lower surface tension.[12,13] Omniphobic materials also demonstrate anti-adhesive properties,[14] which provide plethora applications such as anti-biofouling,[15] and anti-icing.[16] In turn, wettability patterning, based on omniphobic surface structuring, introduces selective adhesion of liquids [17,18] and living cells.[11] Thus, omniphobic–omniphilic structured surfaces can be used as adhesive patterns. Selective adhesion on wettability patterns was used in fabrication of solid patterns.[19] These approaches were shown to produce freestanding microparticles of solid functional materials of defined shapes and sizes, and thus have a vast variety of applications from microengineering to drug delivery.[20] Nevertheless, only few methods of solid structures fabrication rely on wettability patterns. Most of them are based on the use of molds to form the solid into the desired shape and size.[21–23]

Here, we have produced patterns of porous polymethacrylates with different surface chemistry and porosity by using patterns of GPOSS-PDMS. We have shown that the shape and size of the obtained polymethacrylate structures can be predefined by the choice of the GPOSS-PDMS pattern. The patterning did not cause significant changes in the wettability of the omniphobic surface according to the static contact angle and contact angle hysteresis measurements. Thus, a new pattern with a greater difference in wettability of the areas was produced in the process. Discontinuous dewetting of liquids with different surface tensions (water, DMSO, DMF, and hexadecane) was demonstrated. We also performed cell patterning using A549 cells. It was shown that poly(2-hydroxyethyl methacrylate-co-ethylene dimethacrylate) (HEMA-EDMA) application increased the adhesion of cells confined within the omniphilic spots. Thus, less cells were observed outside the omniphilic spots on HEMA-EDMA modified patterns than on unmodified GPOSS-PDMS patterns.

2. Results and Discussion

2.1. Preparation of Porous Methacrylate Patterns Using GPOSS-PDMS Adhesion Patterns

To structure surface adhesive properties, we employed GPOSS-PDMS omniphobic material[24] to obtain patterns by using photolithography.[11] In brief, GPOSS monomers were modified with monoamino-functionalized PDMS to produce surfactant monomer molecules (GPOSS-PDMS). This mixture, in a polar solvent, was spin-coated onto the substrate, dried to remove the solvent, and then polymerized using photolithography. Before polymerization, the surfactant molecules concentrate at the liquid-air interface, resulting in the polymer's low surface energy and omniphobicity. We studied the relationship between spin-coating parameters and GPOSS-PDMS layer thickness. The precursor solution was spin-coated at 1000 rpm for 1 min to achieve a 500 ± 20 nm thin film, sufficient for the required photolithography resolution. Photolithography of GPOSS-PDMS was performed by exposing the thin layer through a glass chromium photomask using a 250 W high pressure mercury vapor lamp for 7 min, with the lamp positioned 10 cm from the sample. Acetone was chosen as the developing agent because it effectively dissolved the unpolymerized GPOSS-PDMS without affecting wettability characteristics of the polymer surface.

To prepare the polymethacrylate pattern, the precursor solution, consisting of methacrylate monomer, crosslinker, photoinitiator, and porogenic solvent, was polymerized between two glasses, one of which was precoated with the GPOSS-PDMS pattern (**Figure 1A**). The second glass was activated by aging in sodium hydroxide and hydrochloric acid solutions (see experimental section (Section 4)). After irradiation with ultraviolet light, the substance between the slides became cloudy, indicating the polymerization and phase separation processes. After separating the glass slides with a scalpel, we observed a separation of the polymer film. A thin polymer layer was applied to the wettable areas of the sample, while the main part of the porous polymer structure remained attached to the activated glass. As a result of the performed operation, the pattern areas, developed during GPOSS-PDMS photolithography, acquired a white tint; previously they were transparent (Figure 1B). When the modified wettable areas were examined under a transmission light microscope, a decrease in their transparency was observed compared to unmodified areas (Figure 1C). Developed areas of different sizes were modified with porous polymethacrylates (Figure 1D–G).

2.2. The Morphology of the Polymethacrylate Patterned Structures

The surface chemistry and roughness of porous polymethacrylates can be controlled by the composition of the precursor solution. 2-Hydroxyethyl methacrylate (HEMA) and 2-(dimethylamino)ethyl methacrylate (DMAEMA) were used as monomers to create polymers with different surface chemistries. To regulate the roughness of the porous structures we varied porogenic solvents (1-nonanol, cyclohexanol, and mixtures of the

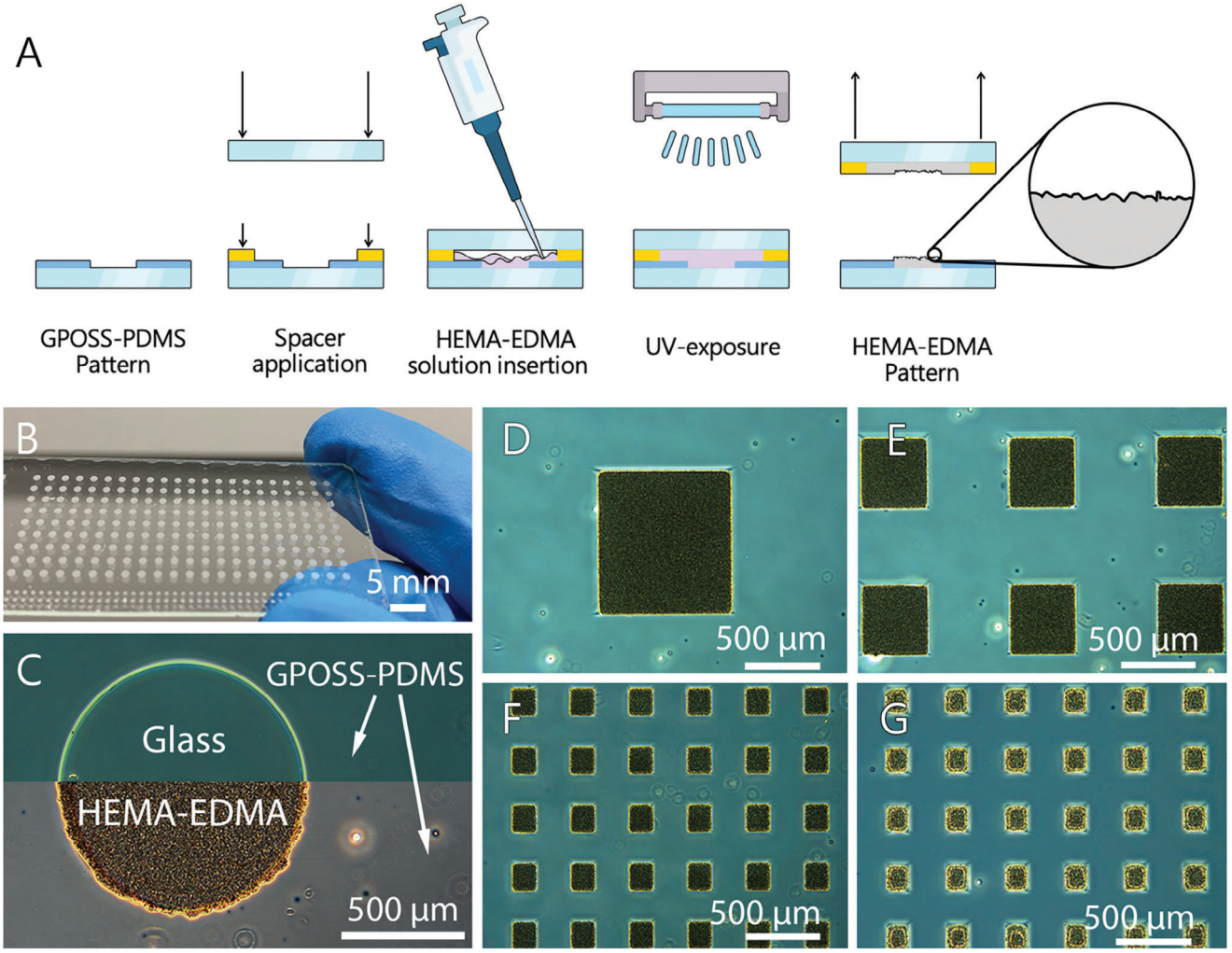

Figure 1. Modification of GPOSS-PDMS wettability patterns using HEMA-EDMA phase separation. A) Scheme of the application of HEMA-EDMA porous structures onto the developed areas of the GPOSS-PDMS pattern. B) Image of the modified wettability pattern (large circles d = 1 mm, small circles d = 0.5 mm). C) Light microscope images of the unmodified (top) and modified (bottom) patterns in comparison, the wettable area of the unmodified pattern demonstrates greater transparency. D–G) Light microscope images of modified areas of various sizes and shapes: D – initial photomask 1×1 mm square, E – 0.5×0.5 mm square, F – 200×200 µm square, G – 100×100 µm square.

two). To inspect the morphology and resolution of the applied polymethacrylate structures, we examined them by scanning electron microscopy (SEM), which revealed that the porous structure is composed of aggregated microparticles (**Figure** 2A,B). As from the SEM images of HEMA-EDMA (Figure 2A,B), aggregates of polymer globules can be seen against a background monolayer of polymer globules of similar size. Thus, the applied HEMA-EDMA structures are heterogeneous at microscale and do not exceed 10 µm in thickness. Cross sectional studies revealed the morphological difference between DMAEMA-EDMA and HEMA-EDMA polymers (Figure 2Ci,ii). DMAEMA-EDMA structures represented 3D polymer monoliths with the same porogenic solvent (1-nonanol) and the amount of crosslinker as was used for HEMA-EDMA. In addition, the DMAEMA-EDMA polymer structures were more even at the microscale, which is due to the smaller size of the polymer globules composing the structure. The average layer thickness for DMAEMA-EDMA was 44.2 ± 1.7 µm. The thicker layers of DMAEMA-EDMA structures may reveal additional high-throughput applications such as solid-phase synthesis and catalysis.

Different globule and pore sizes can be produced in different porogenic solvents, therefore the surface roughness of porous polymethacrylates can be adjusted. We explored the possibility of depositing structures with different HEMA-EDMA globule sizes by changing the porogenic solvent used (Figure S1, Supporting Information). The structures obtained from precursor solutions containing more cyclohexanol were found to consist of smaller polymer globules (Figure 2D,E). It is worth noting that the further increase in the amount of cyclohexanol in the HEMA-EDMA compositions resulted in a further decrease in the average globule size of the produced polymers. However, we were not able to produce patterns of porous polymers in these cases. The entire polymethacrylate film remained attached to the activated glass. At the same time, no traces of porous structures were found within the developed areas of the wettability patterns (Figure S2, Supporting Information). We assume that this effect can be

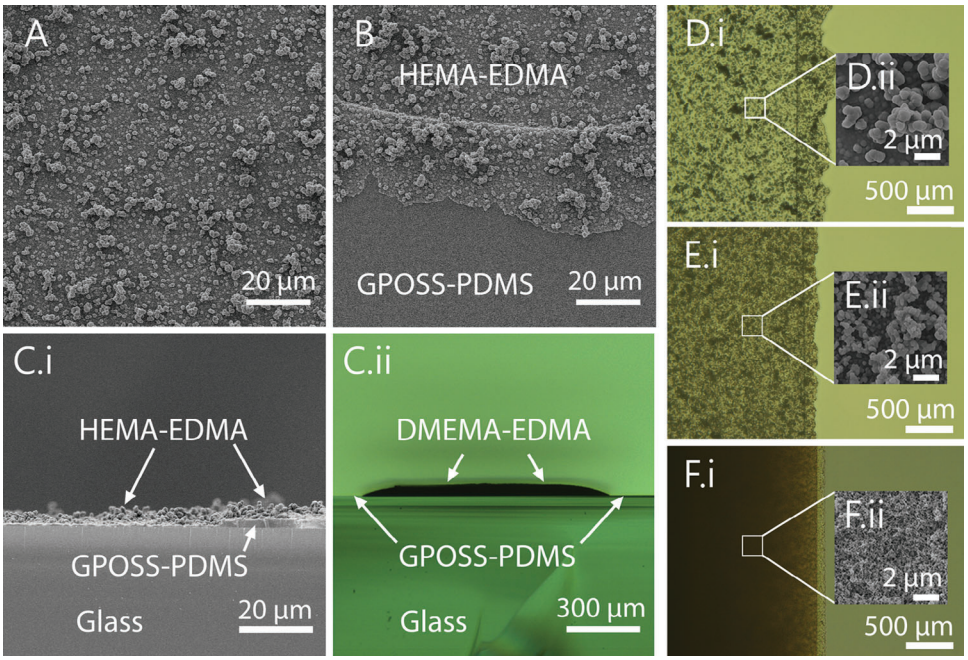

Figure 2. A) SEM image of a developed area after HEMA-EDMA modification. Composition of the precursor solution: HEMA 240 µL, EDMA 160 µL, 1-nonanol 600 µL. The micro-roughness, created by aggregated HEMA-EDMA globules ($R_{av} = 0.81 \pm 0.04$ µm), characteristic to the HEMA-EDMA material, is noticeable. B) SEM image of the boundary between the omniphilic and omniphobic regions. It is noticeable that the HEMA-EDMA structure is partially deposited on the GPOSS-PDMS surface at the pattern boundary. C) (i) SEM image of a cross-section of the wettable area modified with HEMA-EDMA. C) (ii) Light microscope image of a cross-section of the wettable area modified with DMAEMA-EDMA. D) (i). Light microscope image of the porous methacrylate structure border, composition of the precursor solution: HEMA 240 µL, EDMA 160 µL, 1-nonanol 550 µL, cyclohexanol 50 µL. D) (ii) SEM image of the porous methacrylate structure, average globule size ($R_{av} = 0.40 \pm 0.04$ µm). E) (i) Optical microscope image of the porous methacrylate structure boundary, composition of the precursor solution: HEMA 240 µL, EDMA 160 µL, 1-nonanol 450 µL, cyclohexanol 150 µL. E) (ii) SEM image of the porous methacrylate structure, average globule size ($R_{av} = 0.154 \pm 0.006$ µm). F) (i) Light microscope image of the porous methacrylate structure border, composition of the precursor solution: DMAEMA 240 µL, EDMA 160 µL, 1-nonanol 450 µL, cyclohexanol 150 µL F). (ii) SEM image of the porous methacrylate structure.

attributed to the increase of the HEMA-EDMA film integrity with the decrease of the average globule size. We also repeated the patterning procedure with a precursor solution containing no porogenic solvent. In this case, the result was similar to that of the HEMA-EDMA finely porous films. The polymer was not applied to the wettable areas of the pattern, the entire polymer film remained attached to the auxiliary glass (Figure S3, Supporting Information).

During the research, we did not reveal any certain dependence of the applied layer maximum thickness on the polymerization time of HEMA-EDMA between glasses. There was no statistically significant difference between samples obtained during polymerization for 15, and 20 min. However, both former samples had greater thickness than the one polymerized for 10 min (Figure S4, Supporting Information).

Next, we decided to study the resolution of the method in more detail. One can notice that the polymethacrylate layer was partially applied on the omniphobic GPOSS-PDMS material at the boundary of the wettability regions (Figure 2B). The new wettability boundary has a curvature, which, as we discovered, depends on the composition of the methacrylate precursor solution (Figure 2D–F). We noticed that the size of the irregularities at the border correlates with the size of the polymer granules. The fact that the granule size regulates the resolution is expected. This can be explained by assuming that the porous polymethacrylate monolith breaks at the globule connection lines in the separation stage of patterning.

Thus, we have shown the versatility of the method studied by demonstrating the application of structures with different surface chemistry and morphology. We found that HEMA-EDMA compositions produce thin, uneven layers during the application process. In contrast, DMEMA-EDMA compositions produce 3D polymer monoliths with micro-smooth surfaces. We have also shown that HEMA-EDMA patterns with different polymer globule sizes can be obtained. The resolution of the patterning method was shown to depend on polymer globule size.

2.3. Porous Polymethacrylate Modified Wettability Patterns

Wettability difference of the surface areas is essential for droplet array formation, and thus for many of the applications of miniaturized testing. Therefore, we decided to evaluate and compare the wettability of various pattern areas. We measured static contact angles and contact angle hysteresis for several liquids (water, DMSO, DMF, and ethanol) placed on the GPOSS-PDMS surface before and after modification (**Table 1**). The wettability of the omniphobic GPOSS-PDMS surface did not change after modification with HEMA-EDMA according to the measurements. Although we noticed an increase in contact angle hysteresis and a

Table 1. Static contact angles (θ_{st}) (4 µL droplet volume), contact angle hysteresis (CAH) for water, DMSO, DMF, and hexadecane on GPOSS-PDMS and porous polymethacrylate surfaces of the wettability pattern.

Solvent	Surface tension [mN m^{-1}]	θ_{st} GPOSS-PDMS [°]	θ_{st} GPOSS-PDMS (with HEMA-EDMA) [°]	θ_{st} GPOSS-PDMS (with DMAEMA-EDMA) [°]	θ_{st} HEMA-EDMA [°]	θ_{st} DMAEMA-EDMA [°]	CAH GPOSS-PDMS[°]	CAH GPOSS-PDMS (with HEMA-EDMA) [°]	CAH GPOSS-PDMS (with DMAEMA-EDMA)[°]	CAH HEMA-EDMA [°]	CAH DMAEMA-EDMA [°]
Water	72.7	97.9 ± 1.6	95.6 ± 0.8	93.4 ± 3.5	16.3 ± 0.5	spread	15.4 ± 1.6	15.2 ± 2.3	37.8 ± 1.1	–[b]	–
DMSO	43.0	72.4 ± 0.9	71.6 ± 1.4	66.9 ± 1.2	Spread[a]	spread	6.5 ± 0.7	5.3 ± 2.0	27.0 ± 3.5	–	–
DMF	35.3	59.8 ± 0.5	59.6 ± 0.8	51.4 ± 2.4	spread	spread	2.7 ± 0.8	3.5 ± 1.2	25.8 ± 3.2	–	–
Ethanol (96%)	22.8	34.5 ± 1.2	33.6 ± 0.5	23.8 ± 0.7	spread	spread	2.6 ± 0.7	1.7 ± 0.6	17.5 ± 2.8	–	–

[a] Apparent contact angle value is close to 0°; [b] Liquid penetrates the porous structure, so the advancing and receding angles are both close to 0° and the hysteresis cannot be measured.

decrease in static contact angles of liquids placed on the omniphobic surface after DMAEMA-EDMA modification. Despite the slight increase in GPOSS-PDMS wettability, DMAEMA-EDMA patterns could still be used to obtain droplet arrays of water and organic liquids. Although, it is worth noting that some of the low surface tension liquids, such as ethanol (95%), acetone, and isopropanol formed liquid droplet arrays only on HEMA-EDMA modified and unmodified patterns. Thus, herein, porous polymethacrylate patterning represents a new method of adjusting wettability, porosity, and surface chemistry of the developed regions in GPOSS-PDMS patterns.

Significant differences in wettability characteristics between GPOSS-PDMS and porous polymethacrylate surfaces were registered (Table 1) (**Figure 3**A,B). In fact, the porous polymethacrylates prepared in the study demonstrate superwettability with static contact angles close to zero degrees for all liquids tested.

We tested the application of various liquids to HEMA-EDMA and DMAEMA-EDMA patterns by discontinuous dewetting (Figure 3C). The liquids were applied in similar conditions using wettability patterns with square (1 × 1 mm) wettable areas (see experimental section (Section 4)). All the liquids formed droplet arrays on HEMA-EDMA patterns, although ethanol, isopropanol, and acetone did not form droplet arrays on DMAEMA-EDMA patterns (Figure 3D–F).

To summarize the main idea of this section, by demonstrating the inertness of the omniphobic GPOSS-PDMS layer, we have shown that the new microstructuring method for porous polymethacrylates can also be used as a versatile technique to tune the surface chemistry and roughness of the wettability patterns.

2.4. Cell Patterns

We investigated cell growth behavior on patterns with different omniphilic areas using the human lung adenocarcinoma A549 cell line. The experiment included two sample types: an omniphobic pattern without additional coating and a pattern modified with HEMA-EDMA composition (HEMA 240 µL, EDMA 160 µL, 1-nonanol 600 µL).

At the end of the first day of incubation, there were fewer cells on the omniphobic coating of the HEMA-EDMA modified patterns than on the omniphobic coating of the unmodified samples. On average, the number of cells was 61% lower (**Figure 4**Ai,ii). For unmodified patterns the number of cells on the omniphobic coating was 284 ± 67 cells mm^{-2} and for HEMA-EDMA modified samples 174 ± 58 cells mm^{-2}.

To remove cells from the omniphobic coating, we performed the washing step. Due to the different adhesion strength of cells to omniphilic and omniphobic areas, a short incubation in trypsin-Versen solution allowed to detach cells from the GPOSS-PDMS coating of both modified and unmodified patterns. The cells trapped within the omniphilic spots remained (Figure 4Bi,ii). The reduction in the number of cells on the GPOSS-PDMS coating after washing was 87% for the HEMA-EDMA modified patterns and 76% for the unmodified patterns (22 ± 4 cells mm^{-2} and 67 ± 16 cells mm^{-2}, respectively).

On the first day of incubation after washing, the number of cells on the omniphobic coating of unmodified patterns decreased. (Figure 4Ci,ii). For unmodified samples the number of

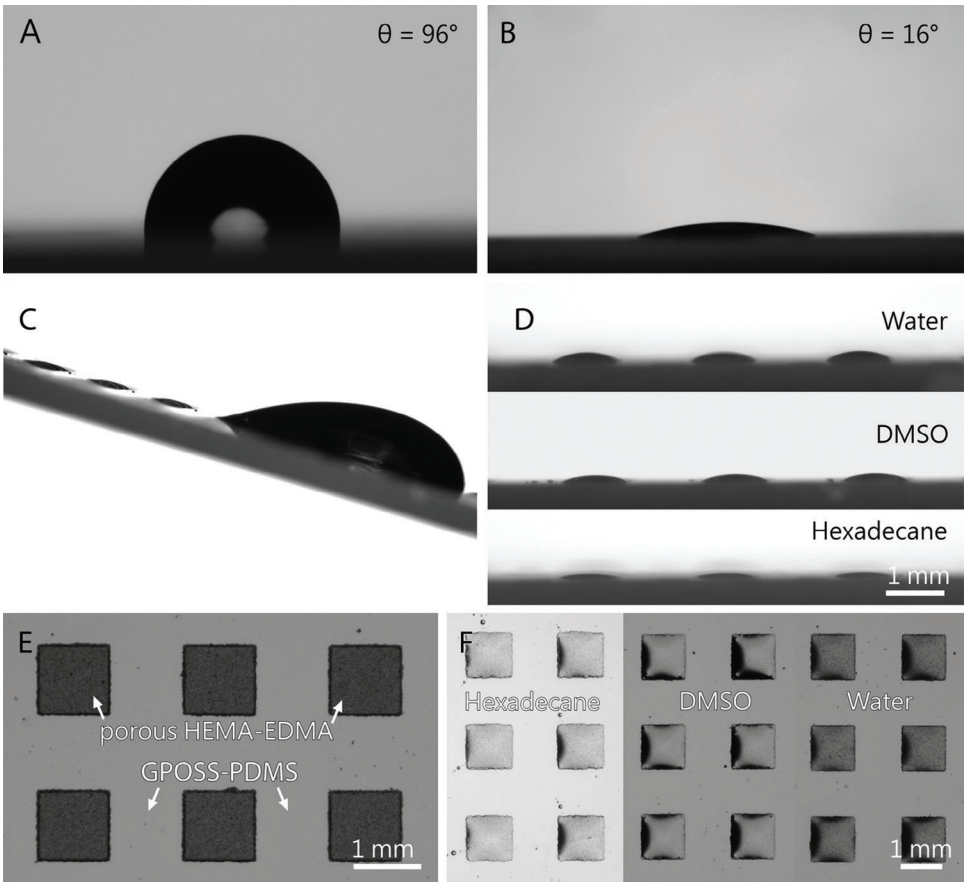

Figure 3. Images of droplet arrays formed on the omniphobic GPOSS-PDMS surface patterned with hydrophilic porous HEMA-EDMA microsquares. Deposition of droplet arrays of various liquids. A) Droplet of water $\nu = 4$ µL on GPOSS-PDMS surface of HEMA-EDMA modified wettability pattern. B) Droplet of water $\nu = 4$ µL on HEMA-EDMA surface of HEMA-EDMA modified wettability pattern. C) Application of DMSO on the HEMA-EDMA modified wettability pattern by discontinuous dewetting. D) Droplet arrays of various liquids applied on the HEMA-EDMA wettability pattern by discontinuous dewetting (side view). Droplet height: water – 0.176 ± 0.021 mm, DMSO – 0.133 ± 0.014 mm, hexadecane – 0.070 ± 0.027 mm. Different droplet heights in experiments with various solvents applied by discontinuous dewetting indicate a difference in droplet volume. E) HEMA-EDMA wettability pattern without solvent applied. F) Droplet arrays of various liquids applied to the HEMA-EDMA wettability pattern by discontinuous dewetting (top view).

cells on the omniphobic coating was 29 ± 7 cells mm^{-2} and for HEMA-EDMA modified samples 15 ± 9 cells mm^{-2}.

On the fifth day of incubation after washing, Hoechst 33 342 staining was performed, and the number of cells was assessed on the omniphobic and omniphilic surfaces of the patterns. The final number of cells on the GPOSS-PDMS coating appeared to be 70% lower on the HEMA-EDMA modified patterns than on the unmodified patterns. For unmodified samples, the average number of cells on omniphobic coating was 17 ± 1 cells mm^{-2} and for HEMA-EDMA modified samples it was 5 ± 2 cells mm^{-2}. At the same time, the number of cells within the omniphilic areas was higher for the HEMA-EDMA modified patterns (Figure 4D(i,ii),E(i,ii)). Specifically, the number of cells on the HEMA-EDMA films was 185% greater than on the unmodified glass omniphilic areas (37 ± 2 cells per spot on the HEMA-EDMA and 20 ± 2 cells per spot on the unmodified glass).

These findings demonstrate that with the new patterning method, it is possible to achieve a significant increase in the number of cells within the patterns while reducing number of cells on the omniphobic part, thereby enhancing the selectivity of cell distribution. This suggests that the GPOSS-PDMS wettability patterns and their HEMA-EDMA modification can be used to control cell growth and distribution, which has significant implications for various biomedical applications.

3. Conclusion

In conclusion, we have introduced a new method for direct and selective deposition of porous polymethacrylate films by using adhesion patterns. The adhesion patterns were obtained by photolithography of GPOSS-PDMS omniphobic material, which was reported earlier. Polymerization-induced phase separation was used to obtain the porosity of the patterned structures. Thus, the precursor solutions of HEMA-EDMA and DMAEMA-EDMA, containing porogenic solvents (nonanol, cyclohexanol), were photopolymerized between the surfaces of a GPOSS-PDMS patterned glass slide and a clean glass slide to produce patterns of porous polymethacrylate films. We have shown that the shape and size of the obtained polymer films can be predefined by the geometry of the omniphobic/repellent GPOSS-PDMS pattern on glass substrates. Thus, methods for obtaining HEMA-EDMA and

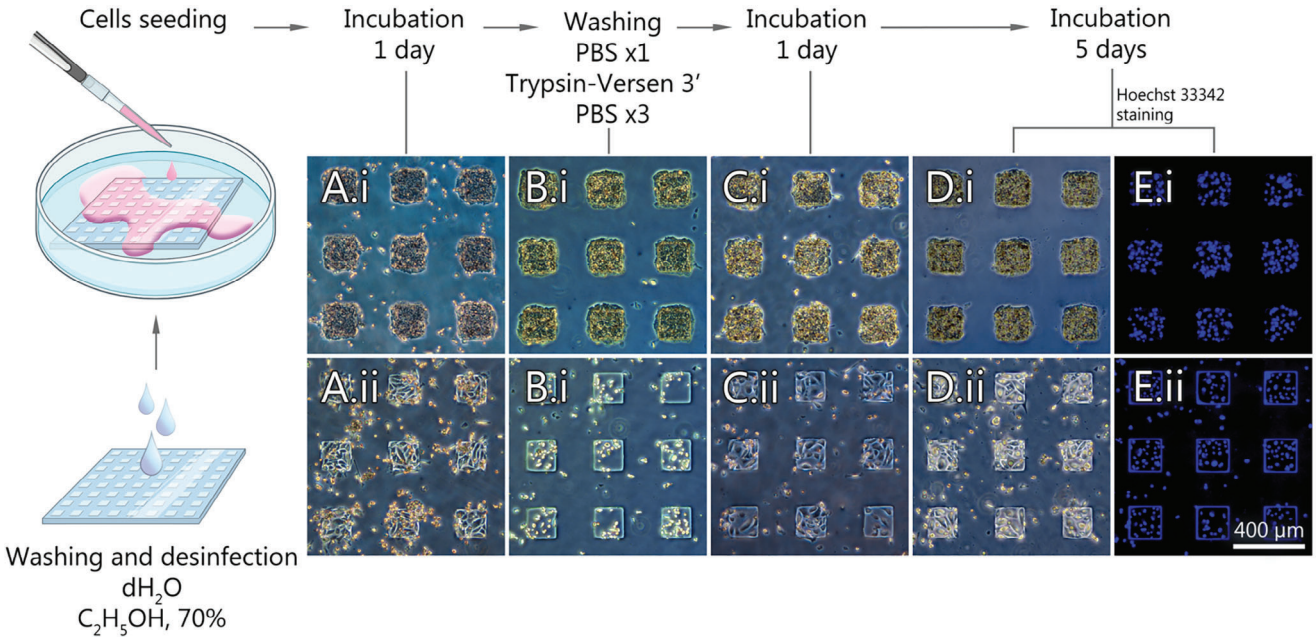

Figure 4. Culturing and patterning of A549 cells on the patterned surface. A) A549 cells on patterns, images after 1 day of incubation. B) Images of cells on wettability patterns immediately after the washing with trypsin-Versen solution. C) Images of cells on wettability patterns 1 day after washing with trypsin-Versen solution. D) Images of cells on wettability patterns on the 5-th day of incubation after washing with trypsin-Versen solution. E) Images of Hoechst 33 342 stained cells on wettability patterns at the 5-th day of incubation after washing with trypsin-Versen solution. Top line (i): HEMA-EDMA modified omniphilic areas. Bottom line (ii): unmodified (glass) omniphilic areas.

DMAEMA-EDMA structures of different shapes (square, circle) and sizes (100-1000 µm) have been described.

We have also demonstrated the patterning for precursor compositions with different monomers (HEMA, DMAEMA) and porogenic solvents (1-nonanol, cyclohexanol, and mixtures of the former). The morphology of the polymer patterns was studied and the selective application of structures with different thickness and roughness was demonstrated. The applied HEMA-EDMA structures were very heterogeneous at the microscale and did not exceed 10 µm in thickness. In contrast with this, the DMAEMA-EDMA structures represented 3D polymer monoliths. The average layer thickness for DMAEMA-EDMA appeared to be 44.2 ± 1.7 µm.

According to the measurements of static contact angles and contact angle hysteresis of various liquids (water, DMSO, DMF, and ethanol) on the GPOSS-PDMS surface before and after the application of the porous polymethacrylate pattern, we found no changes in wettability caused by the operations performed. Thus, a new pattern with greater difference in wettability of the areas was produced in the process. Discontinuous dewetting of liquids of various surface tensions (water, DMSO, DMF, and hexadecane) was demonstrated.

We also performed cell patterning using A549 cells, taking advantage of the significantly different cell adhesion properties of the omniphobic/repellent GPOSS-PDMS background and the hydrophilic porous HEMA-EDMA structures. In the experiment of culturing A549 cells on the surfaces of the patterns, it was shown that the HEMA-EDMA application increased the selectivity of cell adhesion. Thus, fewer cells were observed outside the omniphilic spots on the HEMA-EDMA modified patterns than on the unmodified GPOSS-PDMS patterns. This suggests that the new porous polymethacrylate microstructuring method can be used to control cell growth and distribution, which has significant implications for various biomedical applications.

4. Experimental Section

Chemicals: 3-Glycidyloxypropyl polyhedral oligomeric silsesquioxane (GPOSS) was purchased from Hybrid Plastics (Hattiesburg, MS, USA). Monoaminopropyl-terminated polydimethylsiloxane 18–25 cSt (PDMS-NH_2) was purchased from Gelest (Morrisville, PA, USA). A mixture of triarylsulfonium hexafluoroantimonate (50 wt.% in propylene carbonate), propylene carbonate, 2-hydroxyethyl methacrylate (HEMA), 2-(dimethylamino)ethyl methacrylate DMAEMA, ethylene glycol dimethacrylate, 1-nonanol, cyclohexanol, and 1-hydroxycyclohexyl phenyl ketone were purchased from Sigma–Aldrich (St. Louis, MO, USA). Butyl acetate, ethanol, methanol, hexadecane, DMSO, DMF, acetone, and acetonitrile were used as received from Lenreactive (St. Petersburg, Russia). DMEM culture medium, FBS, PBS, and antibiotics were purchased from Biolot (St. Petersburg, Russia).

Preparation of GPOSS-PDMS Patterns: *Substrate Preparation*: Glass slide activation: commercially available glass slides (76 × 26 mm) were placed in a 1 M solution of sodium hydroxide for 1 h. The slides were then kept in hydrochloric acid (5 wt.%) for 20 min. The glass slides were then thoroughly rinsed with deionized water and dried under air flow. The glass slides were used immediately after activation.

Synthesis of GPOSS-PDMS Colloidal Solution: In a round bottom flask, the GPOSS cage mixture (1 g; 0.75 mmol) was dissolved in butyl acetate (2 mL). PDMS-NH_2 (55 mg, 0.0275 mmol) was then added to the obtained solution. The mixture was heated under reflux at 110 °C for 1.5 h. The reaction mixture containing GPOSS-PDMS and unreacted GPOSS was cooled to room temperature and poured into acetonitrile (14 mL). The obtained solution was centrifuged at 1.60×10^4 g for 1 min. The supernatant was then separated by decantation.

Precursor Solution Preparation: For pattern fabrication, the precursor solution was prepared as a mixture of 60 mg of GPOSS,

1 mL of GPOSS-PDMS colloidal solution prepared in the previous step, 200 µL of propylene carbonate, and 10 µL of photoinitiator solution (mixed salts of triarylsulfonium hexafluoroantimonate 50% by weight in propylene carbonate).

Photolithography Process: *Coating Application*: To fabricate patterns, a precursor solution (500 µL) was evenly spread on an activated glass slide (76 × 26 mm size) and then spin-coated with POLOS SPIN150i at 1000 rpm for 1 min.

Photolithography: At the end of the spin-coating process, a glass slide was placed on a heating plate and dried at 80 °C for 10 min. Then, the dried coating was irradiated with a high-pressure mercury vapor lamp (250 W, wavelength range from 254 to 579 nm, 6.9 mW × cm^{-2} at a wavelength of 365 nm, 10 cm distance between the source and the substrate) for 8 min using a lime-glass-chromium photomask (the thickness of the metal mask was ≈100 nm). The pattern was developed in acetone for 30 s.

Porous Polymethacrylate Patterning: *Preparation of HEMA-EDMA Precursor Solution*: To prepare the HEMA-EDMA precursor solution, 7 mg of photoinitiator (1-hydroxycyclohexyl phenyl ketone) was dissolved in porogenic solvent (composition 1:600 µL of 1-nonanol; composition 2:550 µL of 1-nonanol and 50 µL of cyclohexanol; composition 3:450 µL of 1-nonanol and 150 µL of cyclohexanol). 240 µL of monomer (HEMA) and 160 µL of crosslinker (EDMA) were added to the resulting solution. The solution was used within 1 day after preparation.

Preparation of the DMAEMA-EDMA Precursor Solution: To prepare the DMAEMA-EDMA precursor solution, 7 mg of photoinitiator (1-hydroxycyclohexyl phenyl ketone) was dissolved in 600 µL of 1-nonanol. 240 µL of monomer (DMAEMA) and 160 µL of crosslinker (EDMA) were added to the resulting solution. The solution was used within 1 day after preparation.

Porous Polymethacrylate Patterning: To obtain patterns of porous polymethacrylates, precursor solutions prepared earlier were injected between the activated glass and the GPOSS-PDMS pattern, secured with 100 µm thick double-sided polyimide tape (Figure 1A). The solution placed between the glasses was irradiated with a high-pressure mercury gas lamp (250 W, wavelength range from 254 to 579 nm, 6.9 mW cm^{-2} at a wavelength of 365 nm) for 20 min. The GPOSS-PDMS patterned glass was located closer to the radiation source. After irradiation, a significant clouding of the mass between the glasses was noticeable. The glasses were separated using a scalpel. The modified GPOSS-PDMS pattern was washed with isopropyl alcohol to remove any remaining precursor solution and dried at room temperature without further treatment.

Cell Experiments: The human lung adenocarcinoma cell line A549 was used to evaluate cell adherence to the patterns. The GPOSS-PDMS patterned slides were washed with distilled water, sterilized with 70% ethanol for 20 min, and then placed in sterile 35 mm Petri dishes in laminar hood to dry. Then, 2 mL of the culture medium (DMEM + 10% FBS + Pen/Strep) was added to the Petri dish. Further, 1 mL of A549 cell suspension (C = 1.7 × 10^5 cells mL^{-1}) was added and the dish was placed in an incubator (37 °C, 5% CO_2) for 24 h. After one day of incubation, the slides were washed according to the following protocol: culture medium was removed, samples were washed with 2 mL of PBS, and then incubated in trypsin-Versen (1:1) solution for 3 min. Next, the slides were triple rinsed with PBS and placed in culture medium, the dish was placed in an incubator. After 5 days of incubation, the cells were stained with Hoechst 33 342 for 20 min, then the slides were washed with PBS. The cells were visualized under a Leica DMi 8 microscope (Leica Microsystems CMS, Wetzlar, Germany).

Characterization Methods: The surface of the patterned slides was characterized by contact angle measurements using a Drop Shape Analyzer DSA25 (Krüss GmbH, Hamburg, Germany). The apparent static contact angles were measured using the Young-Laplace fitting method by applying 4 µL droplets of various liquids (ethanol, hexadecane, DMF, DMSO, and water) on omniphilic or omniphobic areas. Advancing contact angles were measured with the following method.[25] Briefly, a 2 µL droplet of the liquid being tested was applied to the surface of a sample. The source needle was placed halfway inside the droplet from the perspective of the camera in the middle of the droplet. Subsequently, 1 µL of the liquid was dispensed at a flow rate of 0.05 µL s^{-1}. In the last stage, the dispensation of an 8 µL volume at a flow rate of 0.05 µL s^{-1} was recorded. The recorded images were analyzed. The final advancing contact angle was calculated as the average of the contact angle values obtained from each image in the measurement. The receding contact angles were measured according to the following method.[25] Briefly, the dispenser needle was placed close to the sample surface without touching it. A 13 µL droplet was applied to the surface of the sample at a flow rate of 2 µL s^{-1}. Subsequently, 2 µL of the liquid was removed from the droplet at a flow rate of 0.05 µL s^{-1}. In the last stage of the measurement, the liquid was removed at a flow rate of 0.05 µL s^{-1} until complete removal. Images recorded during the last stage of the measurement were analyzed. The final receding contact angle was calculated as the average of the contact angle values obtained from each image in the measurement. Scanning electron microscopy (SEM) analyses were performed using a VEGA 3 SBH (Brno, Czech Republic).

Statistical Analysis: All data is shown as mean±marginal error of the mean. ANOVA was used to check statistical differences in measured values. In case the sample distribution was not normally distributed, the Kraskell–Wallis test and Dunn's post-hoc test with Bonferoni corrections were applied. In the case of normal distribution, the Welch test with a post-hoc Games-Howell test was applied. Statistical differences were accepted at the level of $p < 0.05$.

Supporting Information

Supporting Information is available from the Wiley Online Library or from the author.

Acknowledgements

The work of D.D.K., I.M.L., E.G.S., and A.Y.P. was supported by the national project "Science and Universities", project No. FSER-2022-0008.

Open access funding enabled and organized by Projekt DEAL.

Conflict of Interest

The authors declare no conflict of interest.

Data Availability Statement

The data that support the findings of this study are available from the corresponding author upon reasonable request.

Keywords

cell patterning, omniphobic surfaces, photolithography, polymerization induced phase separation, porous polymethacrylate, wettability patterns

Received: June 28, 2024
Revised: August 10, 2024
Published online:

[1] C. S. Chen, M. Mrksich, S. Huang, G. M. Whitesides, D. E. Ingber, *Science* **1997**, *276*, 1425.
[2] E. Ueda, P. A. Levkin, *Adv. Mater.* **2013**, *25*, 1234.
[3] W. Feng, E. Ueda, P. A. Levkin, *Adv. Mater.* **2018**, *30*, 1706111.
[4] K. Yang, J. Shi, L. Wang, Y. Chen, C. Liang, L. Yang, L. N. Wang, *J. Mater. Sci. Technol.* **2022**, *99*, 82.
[5] M. Jaggy, P. Zhang, A. M. Greiner, T. J. Autenrieth, V. Nedashkivska, A. N. Efremov, C. Blattner, M. Bastmeyer, P. A. Levkin, *Nano Lett.* **2015**, *15*, 7146.

[6] M. He, Y. Zeng, X. Sun, D. J. Harrison, *Electrophoresis* **2008**, *29*, 2980.
[7] W. Feng, L. Li, E. Ueda, J. Li, S. Heißler, A. Welle, O. Trapp, P. A. Levkin, *Adv. Mater. Interfaces* **2014**, *1*, 1400269.
[8] W. Feng, L. Li, C. Yang, A. Welle, O. Trapp, P. A. Levkin, *Angew. Chem.* **2015**, *127*, 8856.
[9] L. Li, J. Li, X. Du, A. Welle, M. Grunze, O. Trapp, P. A. Levkin, *Angew. Chem., Int. Ed.* **2014**, *53*, 3835.
[10] M. Hirtz, W. Feng, H. Fuchs, P. A. Levkin, *Adv. Mater. Interfaces* **2016**, *3*, 1500469.
[11] D. D. Kartsev, A. Y. Prilepskii, I. M. Lukyanov, E. G. Sharapenkov, A. V. Klaving, A. Goltaev, A. Mozharov, L. Dvoretckaia, I. Mukhin, P. A. Levkin, *Adv. Mater. Interfaces* **2023**, *10*, 2300156.
[12] Z. Chu, S. Seeger, *Chem. Soc. Rev.* **2014**, *43*, 2784.
[13] M. A. Samaha, M. Gad-el-Hak, *Phys. Fluids* **2021**, *33*, 071301.
[14] X. Guo, Y. Di, Q. Liang, P. Li, J. Lv, Y. Tian, Q. Li, L. Jiang, C. Xu, Z. Zhang, *ACS Appl. Mater. Interfaces* **2023**, *15*, 17245.
[15] H. J. Cox, C. P. Gibson, G. J. Sharples, J. P. S. Badyal, *Adv. Eng. Mater.* **2022**, *24*, 2101288.
[16] W. Niu, G. Y. Chen, H. Xu, X. Liu, J. Sun, *Adv. Mater.* **2022**, *34*, 2108232.
[17] I. You, T. G. Lee, Y. S. Nam, H. Lee, *ACS Nano* **2014**, *8*, 9016.
[18] W. Feng, L. Li, X. Du, A. Welle, P. A. Levkin, *Adv. Mater.* **2016**, *28*, 3202.
[19] M. Tsotsalas, H. Maheshwari, S. Schmitt, S. Heißler, W. Feng, P. A. Levkin, *Adv. Mater. Interfaces* **2016**, *3*, 1500392.
[20] A. Laromaine, T. Tronser, I. Pini, S. Parets, P. A. Levkin, A. Roig, *Soft Matter* **2018**, *14*, 3955.
[21] Z. Nie, E. Kumacheva, *Nat. Mater.* **2008**, *7*, 277.
[22] E. F. Demir, C. I. Kuru, M. Uygun, D. Aktaş Uygun, S. Akgöl, *J. Biomater. Sci., Polym. Ed.* **2018**, *29*, 344.
[23] Z. Ge, P. R. Girguis, C. R. Buie, *Lab Chip* **2016**, *16*, 480.
[24] K. Zhang, S. Huang, J. Wang, G. Liu, *Angew. Chem.* **2019**, *131*, 12132.
[25] T. Huhtamäki, X. Tian, J. T. Korhonen, R. H. A. Ras, *Nat. Protoc.* **2018**, *13*, 1521.